Environmental Science and Pollution Research (2018) 25:17300–17309
https://doi.org/10.1007/s11356-018-1907-4

RESEARCH ARTICLE

Reductive decolorization of azo dyes via in situ generation of green tea extract-iron chelate

Ling Yu[1,2,3] · Yewen Qiu[1,4] · Yang Yu[5] · Shanquan Wang[1,2,3]

Received: 1 February 2018 / Accepted: 28 March 2018 / Published online: 13 April 2018

Abstract

In this study, rapid decolorization of azo dyes was achieved by in situ-generated green tea extract-iron (GTE-Fe) chelate for the first time. When changing reaction conditions from the aerobic condition to the anaerobic condition, the decolorization efficiencies of two azo dyes, i.e., acid orange 7 (AO7) and acid black 1 (AB1), increased from 46.38 and 83.17 to 90.13 and 95.37%, respectively. The recalcitrant AO7 was then selected as the targeting pollutant in subsequent optimization and mechanism studies. Experimental evidences showed that the initial concentrations of AO7, Fe(III), and GTE are the key factors to optimize the decolorization efficiency. Further characterization studies by spectroscopic analysis, including FESEM, FTIR, and XPS, suggested that the major mechanism of AO7 decolorization is the nucleophilic attack of the oxygen in green tea polyphenols (GTP), and this attack could be facilitated by the organometal chelation. This study provided an efficient and environmental friendly strategy to decolorize azo dyes via in situ generation of the GTE-Fe chelate, as well as its mechanistic insights, shedding lights on in situ remediation of azo dye pollution.

Keywords Green tea extract-iron chelate · Decolorization · Azo dye · Green tea polyphenols · In situ generation

Introduction

Azo dyes as a class of aromatic compounds with a nitrogen double bond (–N=N–) are widely used in textile dyeing, paper printing, cosmetic, and other industries (Fang et al. 2013; Stolz 2001), accounting for > 70% of total produced dyestuffs (Rawat et al. 2016). Direct discharge of dyeing wastewater into environment raises public concerns due to ecotoxicities and their colorization of receiving waters (Cui et al. 2016b; Lee and Pavlostathis 2004; Pagga and Brown 1986). In azo dye degradation process, decolorization via destroying the nitrogen double bond (or azo bond) is the primary and rate-limiting step (Rathod et al. 2017). Thus, development of an efficient decolorization method is essential for improving azo dye removal efficiency from dyeing wastewater.

The azo dye decolorization by breaking the azo bond is a reductive process, involving four-electron transfer per azo bond (Cui et al. 2016a). Recently, microbial reductive decolorization of azo dyes has been investigated using functional microorganisms and their enzymes (Amjad Ali and Qayyum 2007; Fu and Viraraghavan 2001; Li et al. 2015). These microorganisms could reductively decolorize azo dyes via bond cleavage by utilizing reducing equivalents (e.g., NADH) generated from their catabolic process (Imran et al. 2016). However, the low reaction rate and the toxicity of azo dye molecules to microorganisms hinder its application. By contrast, chemical reductive process could efficiently and rapidly decolorize azo dyes. For example, nanoscale zero valent iron

Responsible editor: Bingcai Pan

Electronic supplementary material The online version of this article (https://doi.org/10.1007/s11356-018-1907-4) contains supplementary material, which is available to authorized users.

✉ Shanquan Wang
wangshanquan@mail.sysu.edu.cn

[1] School of Environmental Science and Engineering, Sun Yat-Sen University, Guangzhou 510275, China

[2] Environmental Microbiome Research Center, Sun Yat-Sen University, Guangzhou 510275, China

[3] Guangdong Provincial Key Laboratory of Environmental Pollution Control and Remediation Technology, Guangzhou 510275, China

[4] Present address: School of Environmental Science and Engineering, Shanghai Jiao Tong University, Shanghai 201100, China

[5] Guangdong Key Laboratory of Environmental Pollution and Health, and School of Environment, Jinan University, Guangzhou 510632, China

(nZVI) was found to be able to destroy the azo bond in disperse red one effectively (Barreto-Rodrigues et al. 2016).

Polyphenols are well known as antioxidants and constitute the most interesting group of green tea extract (GTE) components. Several epidemiological studies have verified that polyphenols have beneficial effects on human health (Serafini et al. 1996; Zaveri 2006). Extensive studies have investigated the antioxidant properties of the polyphenols. As a result, radical scavenging and iron metal chelating are the main mechanism (Grinberg et al. 1997; Melidou et al. 2005; Nanjo et al. 1996; Salah et al. 1995). Polyphenols could be easily deprotonated at acidic condition in the presence of iron and form very stable chelate. Iron ions that possess octahedral geometry can coordinate up to three polyphenol groups (Perron and Brumaghim 2009).

Thereafter, GTE has been widely applied as reducing agents to synthesize nano-sized particles, including silver, iron, and gold nanoparticles, owing to its reducing capacity (Huang et al. 2014; Moulton et al. 2010; Nune et al. 2009). Also exploited the iron metal chelating mechanics, the reduction of graphene oxide sheets by green tea polyphenols could be improved in the presence of iron, achieving a comparable performance with that of hydrazine (Akhavan et al. 2012). Nonetheless, the potential application of green tea polyphenols in the decolorization of azo dyes has not yet been reported. In addition, the possible synergistic decolorization mechanism of green tea polyphenols and iron ions remains elusive.

In situ generation of decolorization material could reduce the operation cost, and few studies on the anaerobic decolorization process have been reported. In this study, we investigated the decolorization of azo dyes by in situ-generated GTE and iron chelate (GTE-Fe) under both aerobic and anaerobic conditions, as well as the major affecting parameters and their optimization for azo dye decolorization. The mechanistic reaction for azo dye decolorization was further proposed. Compared with other technologies, this method is competitive due to low cost, rapid decolorization rate, ease in operation, and environmental friendly.

Materials and methods

Chemicals and materials

Green tea was purchased from Hangzhou Yijiangnan Tea Co., Ltd. (China). High-purity nitrogen gas was purchased from Foshan MS Messer Gas Co., Ltd. (China). Ferric chloride hexahydrate ($FeCl_3 \cdot 6H_2O$), ferrous chloride tetrahydrate ($FeCl_2 \cdot 4H_2O$), acid orange 7 (AO7, $C_{16}H_{11}N_2NaO_4S$), acid black 1 (AB1, $C_{22}H_{14}N_6Na_2O_9S_2$), and all other chemicals were in analytical grade and purchased from Sinopharm Chemical Reagent Co., Ltd. (China). Deionized (DI) water used in all experiments was obtained from Heal Force SMART-P System (China).

In situ decolorization experiments

In the aerobic system, the GTE stock solution was prepared by adding 6 g of finely grinded GT powder in 150 mL of deionized water at 80 °C for 1 h. The GTE stock solution was then cooled down to room temperature for further experiments. The ferric chloride and ferrous chloride stock solution were prepared with the concentration of 30 mg-Fe/L. Then, certain amount of the GTE stock solution and iron chloride stock solution was added into the azo dye-contaminated water together for in situ decolorization.

In the anaerobic system, the deoxygenated water was first prepared by boiling the deionized water for 20 min under N_2 purge of 1 psi with reflux condensation. Subsequently, to prepare the stock solutions, 6 g-GT, certain amount of ferric chloride, ferrous chloride, and azo dyes was added into 200-mL serum bottle together with 150-mL deoxygenated water under N_2 purge of 5 psi using an anaerobic platform and closed with a butyl rubber stopper with a crimped metal seal. The sealed serum bottle with GT was kept into 80 °C water bath for 1 h and then cooled down to room temperature for further experiments. Finally, the GTE stock solution and 30 mg-Fe/L iron chloride stock solution were added into the azo dye-contaminated water successively by syringe with needle for in situ decolorization (the detailed reaction conditions for each experiment were indicated in figure legends). The syringe with needle was deoxygenated by nitrogen flush prior to use. Solution pH was not controlled during the decolorization process. Samples were taken at time intervals, and the azo dye concentration was analyzed using UV spectrophotometer. All the experiments were set up in duplicate.

Analytical techniques

The azo dye concentrations were measured by UV-vis spectrophotometer (Shanghai Metash Instruments Co., Ltd., China). The UV absorbance reading for AO7 and AB1 was, respectively, taken at wavenumber (λ) of 484 and 625 nm according to the results of full-range scanning. The dye concentration was calculated using calibration curves for each dye. As shown in Fig. S1, the calibration curves were built by detecting the UV absorbance of different dye solutions with known concentrations.

The decolorization efficiency (η) was calculated according to Eq. 1 as below:

$$\eta = \frac{C_0 - C_t}{C_0} \times 100\% \quad (1)$$

where C_0 (mg/L) is the initial concentration of dye solution and C_t (mg/L) is the concentration of dye solution at time interval t.

Characterization

The samples were washed by DI water for at least three times and then freeze dried for characterization analysis. The morphology of GTE-Fe was observed by field emission scanning electron microscopy (FESEM, JEOL, JSM-6330F, Japan). The samples were sputter coated with a thin layer of platinum to improve conductivity.

Fourier transform infrared spectroscopy (FTIR) and X-ray photoelectron spectroscopy (XPS) were used to explore the interaction between GTE-Fe and AO7. FTIR spectra of samples were acquired with a Thermo-Fisher FTIR spectrometer (Nicolet NXR 9650). The background was automatically subtracted from the sample spectra. The spectra were collected in the wavenumber range of 40–4000 cm^{-1} at a resolution of 4 cm^{-1} by co-adding 32 scans and plotted in the same scale on the transmittance axis. XPS study of GTE-Fe was conducted using a spectroscope (Shimadzu, Kratos XPS System-AXIS His-165 Ultra, USA) equipped with a monochromatized Al Kα X-ray source (1486.71 eV), which works at 150 W, 15 kV, and 10 mA and base pressure of 3×10^{-8} Torr in the analytical chamber. To compensate for charging effect, C 1s signal of an adventitious carbon at a binding energy (BE) of 284.6 eV was used as reference to correct all XPS spectra. The XPS results were collected in binding energy form and fitted using a non-linear least-square curve fitting program (XPS PEAK41 software).

Bridging effects of metal ions

The potential bridging effect of metallic cations on azo dye decolorization was investigated by replacing iron ions with calcium ions. The concentration of calcium ions was 0.357 g-Ca/L (8.92 mM) equal to the molar concentration of iron ions. Other procedure was the same as the anaerobic in situ decolorization experiment.

Results

Decolorization of azo dyes

Decolorization under aerobic and anaerobic conditions

AO7 and AB1 were chosen as representatives of azo dyes to investigate their decolorization by in situ-generated GTE-Fe chelate under the aerobic and anaerobic conditions. The chemical structures of the two anionic azo dyes are shown in Table S1. Under open-air conditions, the reductive decolorization of AO7 and AB1 was largely completed in the first 15 min (Fig.1a), and their decolorization efficiencies after 8-h reaction further increased to 46.38 and 83.17%, respectively. By contrast, the azo dye decolorization efficiencies were remarkably improved under the anaerobic condition, achieving 90.13 and 95.37% for AO7 and AB1 after 8-h reaction, respectively (Fig.1b). Considering the recalcitrance of AO7 under the aerobic condition, AO7 was chosen for subsequent optimization experiments and mechanism studies.

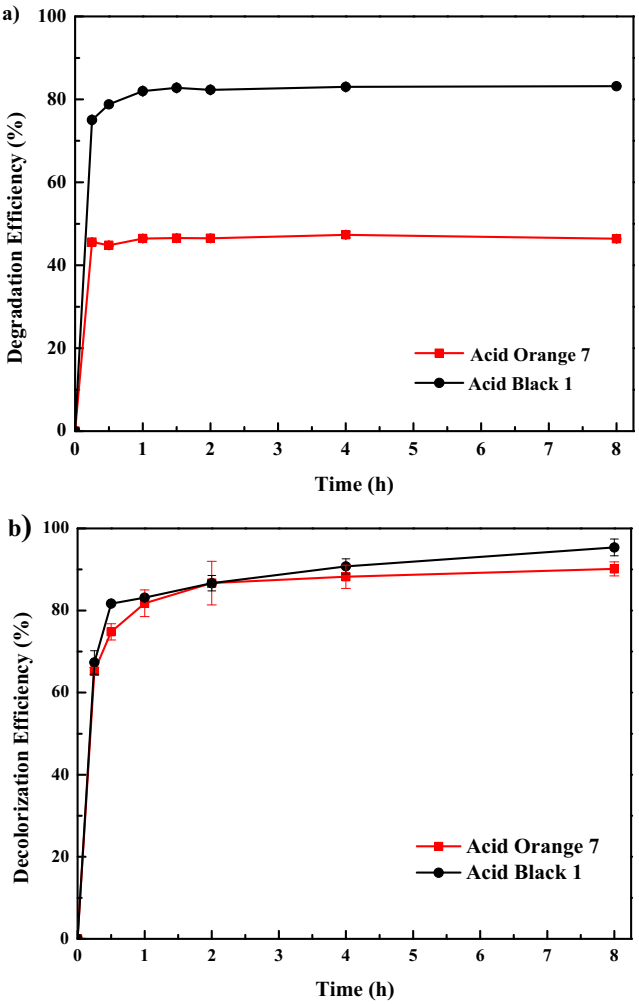

Fig. 1 Decolorization of three different dyes under the aerobic condition (**a**) and the anaerobic condition (**b**). The concentrations of dyes, ferric chloride, and green tea extract (GTE) in the experiment are 50 mg/L, 500 mg-Fe/L, and 6.67 g-GT/L, respectively

Decolorization efficiencies of different decolorants

Experiments on AO7 decolorization by GTE, Fe(III), Fe(II), GTE-Fe(II), and GTE-Fe(III) were performed under the anaerobic condition to compare their decolorization efficiencies (Fig.2). Surprisingly, compared with Fe(II)-containing bottles, i.e., Fe(II) or GTE-Fe(II), higher decolorization efficiencies were observed in Fe(III)-containing bottles, suggesting that iron ions may play other roles rather than providing reducing equivalents for azo dye decolorization. Further comparison of decolorization efficiency of GTE-Fe(II/III) (59.84/90.13%) with these of GTE (30.0%) and Fe(II/III) (9.69/18.93%)

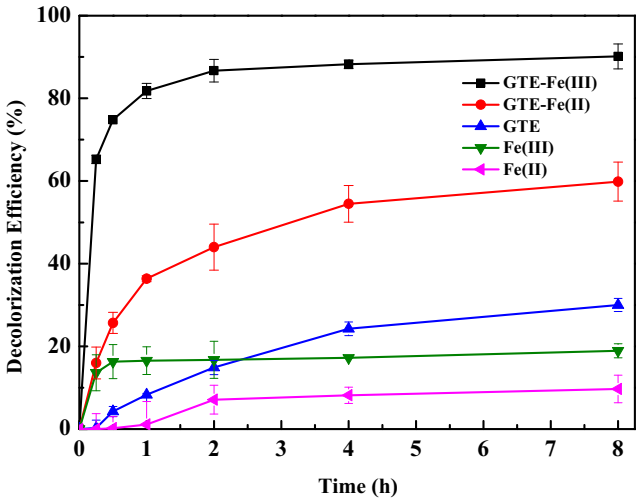

Fig. 2 Decolorization of AO7 with various decolorants. The concentrations of dyes, ferrous/ferric chloride, and green tea extract (GTE) in the experiment are 50 mg/L, 500 mg-Fe/L, and 6.67 g-GT/L, respectively

indicated that the decolorization efficiency of dosing GTE together with iron ions was much higher than simply adding on their respective efficiency. The most possible reason is the generation of organometallic complexes in GTE-Fe(II/III) bottles, which multiplies the decolorization capabilities of GTE and Fe(II/III) as shown in Fig. 2.

Optimization of AO7 decolorization

To optimize AO7 decolorization condition with GTE-Fe(III) in the anaerobic system, the decolorization efficiencies with varied concentrations of GTE, Fe(III), and AO7 were tested (Fig.3). In the optimization of GTE (weight base) concentration, AO7 decolorization efficiency increased with the increase of GT dosage from 1.67 to 6.67 g/L, and further GT addition did not make notable difference in decolorization efficiency (Fig. 3a). The effect of initial Fe(III) concentration (in the range of 0.1–0.9 g/L) on AO7 decolorization showed slightly different trends compared with that of GTE, and the highest decolorization efficiency was observed with the ferric ion dosage of 0.5 g-Fe/L rather than 0.9 g-Fe/L. Therefore, the optimal AO7 decolorization could be achieved under conditions with GTE and Fe(III) dosage of 6.67 and 0.5 g/L, respectively. To further test the optimal AO7 decolorization condition, experiments were conducted with five AO7 concentration gradients (i.e., 10, 50, 100, 200, and 400 mg/L). The highest decolorization efficiency of 94.38% was obtained at the AO7 concentration of 100 mg/L (Fig. 3c).

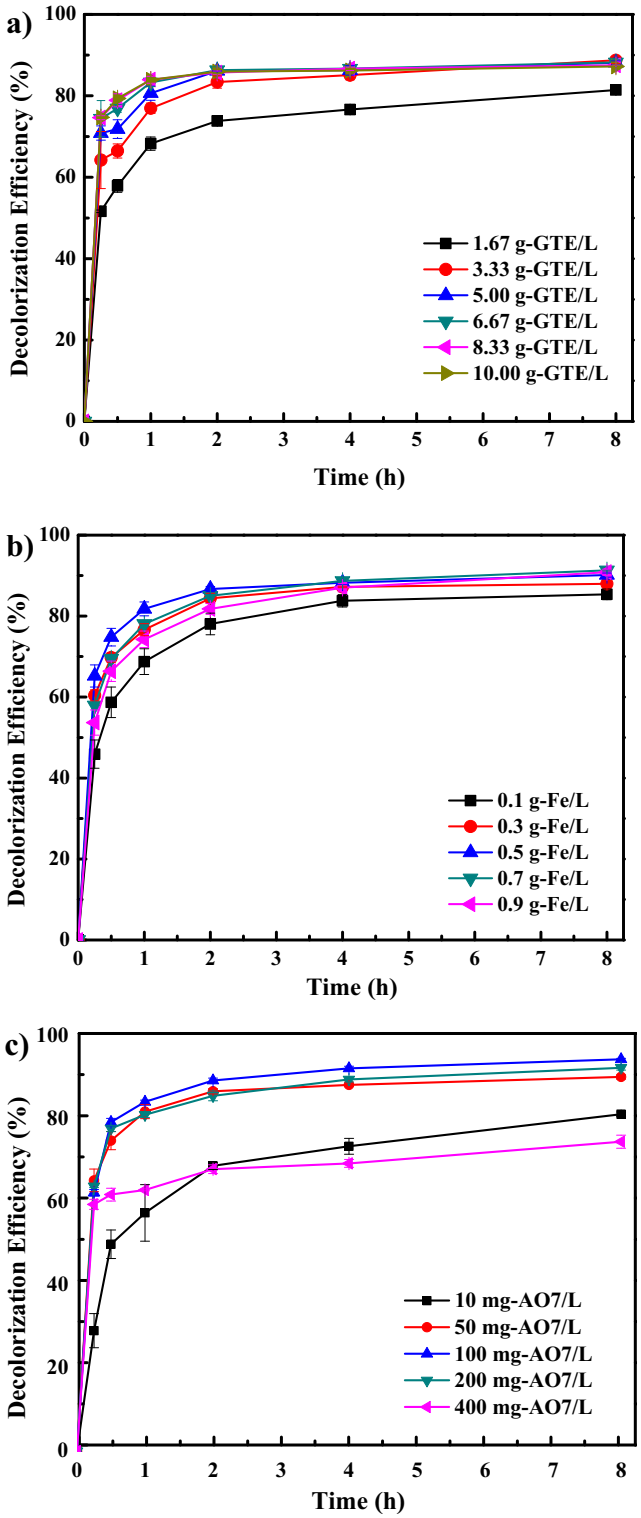

Fig. 3 Effects of GT dosage (**a**) and concentrations of Fe(III) (**b**) and AO7 (**c**) on the efficiency of AO7 decolorization by GTE-Fe(III) chelate

Characterization of in situ-generated GTE-Fe chelate

The surface morphologies of in situ-generated GTE-Fe chelate with and without AO7 treatment were compared with FESEM (Fig.4). After adding Fe(III) into GTE solution under the anaerobic conditions, formation of flocs could be observed, on which GTE-Fe chelate aggregated as spherical nano-sized particles (Fig. 4a). While in the presence of AO7,

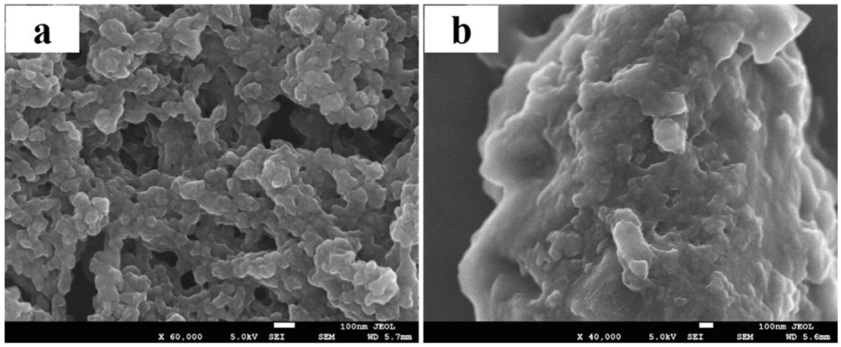

Fig. 4 FESEM characterization of the GTE-Fe chelate before (**a**) and after (**b**) reaction with AO7

the GTE-Fe chelate was showed to stick together with bulk clumps (Fig. 4b).

The surface element distribution of GTE-Fe chelate was determined by XPS spectrum. The wide-scan spectrum (Fig. 5a) showed characteristic peaks of Si, C, N, O, and Fe elements on the surface of GTE-Fe chelate. The appearance of Fe 2p and Fe 2s peaks suggested the chelation of GTE and Fe(III) ions. The Si element could be originated from the glassware used during sample preparation. As shown in Fig. 5b, the high-resolution XPS spectrum of O 1s of GTE-Fe can be divided into three component peaks at binding energies of 531.7, 532.6, and 533.4 eV. According to the XPS database of the National Institute for Standards and Technology (NIST), the three peaks represented Fe–O, C–O, and C=O, respectively (Barth et al. 1988; Beamson and Briggs 1992; Blomquist et al. 1983; Srivastava et al. 1985; Tan et al. 1990). The Fe–O band could be yielded from organometallic Fe compounds. The valence state of iron ions in GTE-Fe was investigated by the Fe 2p XPS spectrum as shown in Fig. 5c. The peak at the lowest binding energy of 709.4 eV and its corresponding satellite peak at 714.2 eV were assigned to Fe(II), while the peak of Fe(III) could be observed at binding energies of 711.3 eV (Wilson and Langell 2014). These results suggested that Fe(III) was reduced to Fe(II) while chelating with GTE, resulting in two oxidation states of Fe element existing in the GTE-Fe chelate (Biesinger et al. 2011). In addition, the peak at 711.3 eV attributing to Fe–O suggested that the Fe was complexed with O as organoiron (Blomquist et al. 1983). These results further confirmed that iron ions were bonded with GTE via sharing electron pair, forming GTE-Fe chelate.

Decolorization mechanism

The FTIR analysis was employed to identify the interactions among GTE, Fe(III), and AO7 (Fig.6). The results showed that there was no significant difference between FTIR spectra of GTE-Fe with or without AO7, indicating the negligible adsorption of AO7 on GTE-Fe chelate during the dye decolorization process. The characteristic bonds of AO7 could be observed in Fig. 6c. The strong band at 1500 cm^{-1} represented an azo bond vibration or an aromatic ring (C=C) vibration (Vinodgopal et al. 1996). The bands at 1620, 1590, 1550, and 1450 cm^{-1} can be attributed to aromatic skeletal vibrations. Other bonds at 1320, 1120, and 1030 cm^{-1} referred to O–H bending vibrations, aromatic C–N stretching vibration, and C–O–H stretching vibration, respectively (Zhang et al. 2005). Notably, the FTIR spectrum of AO7 was not changed in the presence of Fe(III) ions, suggesting that the removal of AO7 by adding Fe(III) solution was mainly due to the flocculation rather than the cleavage of chromophore of AO7 (azo bond).

The high-resolution XPS spectra of C 1s of GTE-Fe chelate before and after AO7 treatment are shown in Fig.7. The characteristic peak of C 1s was composed of three component peaks at the binding energies of 284.5, 286.3, and 288.3 eV, which were assigned to C=C/C–C/C–H, C–OH, and C=O, respectively (Akhavan et al. 2012). The peak area and relative content of functional bonds in GTE-Fe before and after AO7 treatment are summarized in Table S2. To quantify the changes of GTE-Fe structure during azo dye decolorization, the ratio of C–OH, C=O to C–C peak area was calculated. In contrast to the decrease of C–OH bond in GTE-Fe, the content of C=O bond increased after AO7 treatment (Table 1), suggesting the oxidation of GTE in GTE-Fe chelate during AO7 decolorization. The similar change was observed in the high-resolution XPS spectra of O 1s in GTE-Fe chelate before and after AO7 treatment (Fig. S2b). Based on the results shown in Tables S2 and 1, together with high-resolution XPS spectrum of Fe 2p in GTE-Fe (Fig. S2a), the Fe(II)/Fe(III) ratio decrease (from 1.28 to 0.84) in GTE-Fe after AO7 treatment indicated that Fe(II) in the chelate was partially oxidized to Fe(III) while reducing AO7. These results suggested that Fe(II) ions might also function as nucleophiles to attack azo bonds, although with lower reaction rate compared with deprotonated polyphenols. No change of the intensity in N 1s spectrum in GTE-Fe chelate before and after AO7 treatment was observed (Fig. S2c, Table S2), which further confirmed negligible adsorption of AO7 on the GTE-Fe chelate.

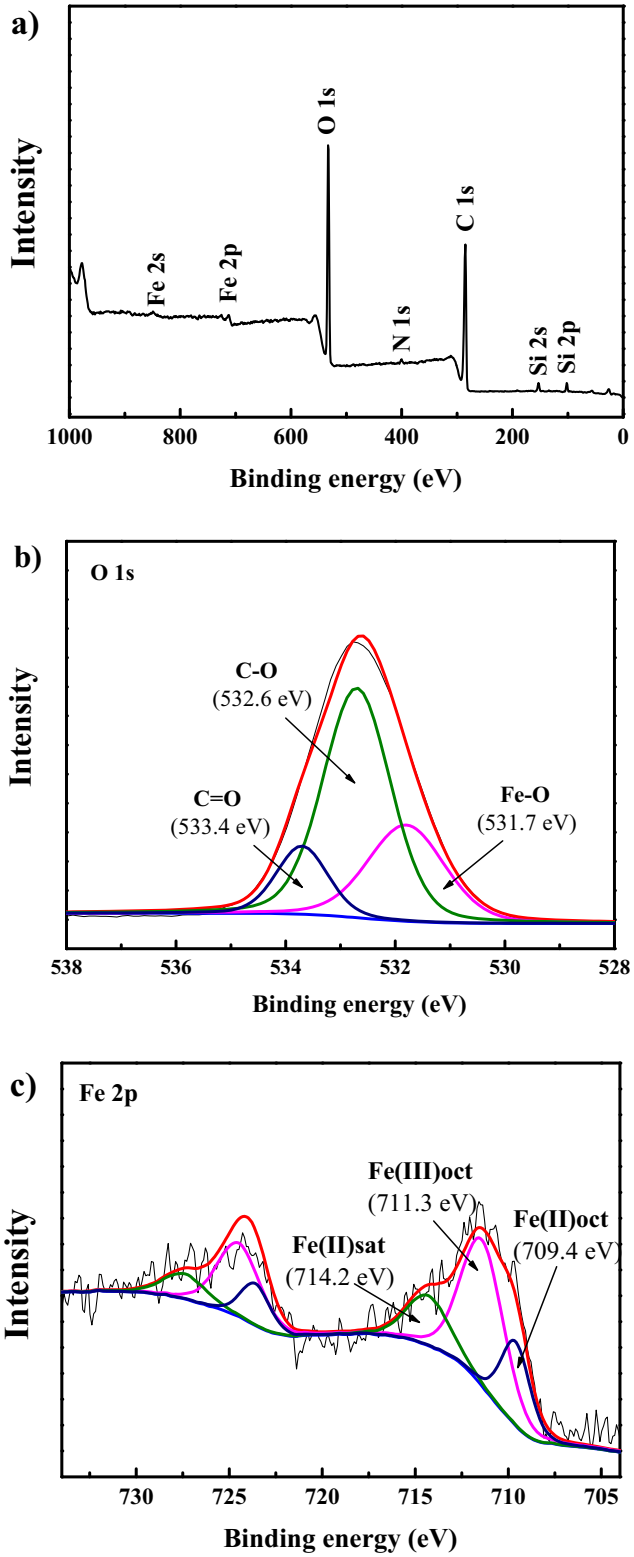

Fig. 5 XPS spectra of GTE-Fe chelate: wide-scan spectrum (**a**) and high-resolution XPS spectra of O 1s (**b**) and Fe 2p (**c**)

Due to the negative charge of AO7 (an anion azo dye) and reactive ingredients of GTE (i.e., polyphenols), the electrostatic repulsion could occur and negatively affect the interaction

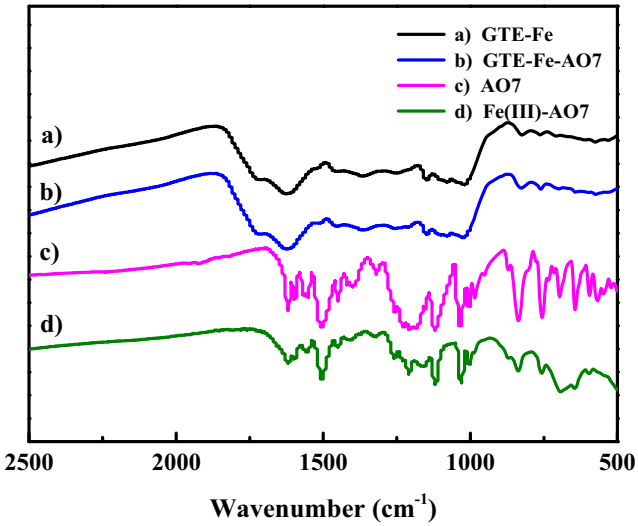

Fig. 6 FTIR spectra of GTE-Fe chelate (**a**), GTE-Fe chelate reacted with AO7 (**b**) and AO7 powder (**c**), and Fe(III) reacted with AO7 (**d**)

between AO7 and GTE ingredients. The addition of Fe(III) or Fe(II) is possible to reduce the negative effects of the electrostatic interaction via double layer compression or interparticle bridging (Aboulhassan et al. 2006). To verify cationic bridging effects, the calcium ions without chelating and reducing ability were employed as a substitute to Fe(III). As shown in Fig.8, the presence of Ca(II) had negligible effect on the decolorization efficiency of AO7 by GTE. Therefore, interparticle bridging of cation ions played a minor role in the improvement of AO7 decolorization. These results showed that the chelation of GTE and metals played the major role in AO7 decolorization. Based on these experimental evidences, we

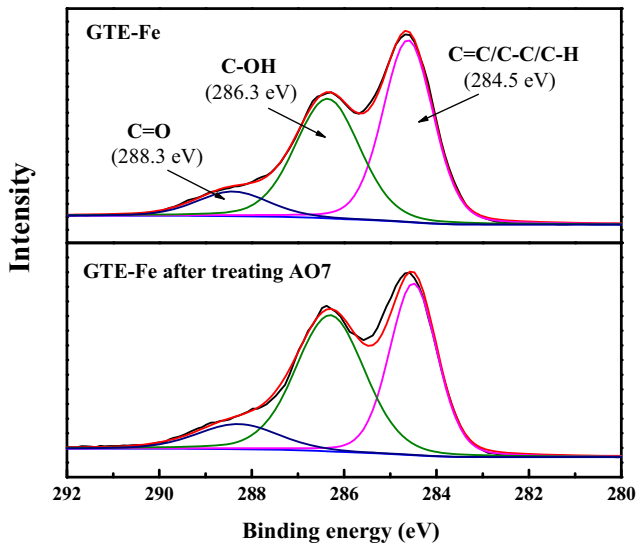

Fig. 7 High-resolution XPS spectra of C 1s of GTE-Fe chelate before and after reaction with AO7

Table 1 Peak area ratios of C–OH/C–C, C=O/C–C, and Fe(II)/Fe(III) in GTE-Fe before and after reaction with AO7

Sample	Peak area (*A*) ratio		
	A_{C-OH}/A_{C-C}	$A_{C=O}/A_{C-C}$	Fe(II)/Fe(III)
GTE-Fe	1.07	0.21	1.28
GTE-Fe-AO7	0.97	0.24	0.84

proposed a mechanistic reaction for azo dye decolorization by in situ-generated GTE-Fe chelate (Eq. 2). Due to the electron-withdrawing property of catechin rings, the two adjacent hydroxyl groups in GT polyphenols can be facilely deprotonated and act as nucleophiles. The azo bonds in AO7 can therefore be cleaved by oxygen in deprotonated polyphenols via nucleophilic attack. Meanwhile, the C–OH bonds in polyphenols were oxidized to C=O bonds. The presence of Fe(III) or Fe(II) ions may accelerate the deprotonating of hydroxyl bonds in GT polyphenols, resulting in a significant improvement in AO7 decolorization. Notably, compared with Fe(II), Fe(III) activated higher percentage of GT polyphenols due to its stronger deprotonation capability.

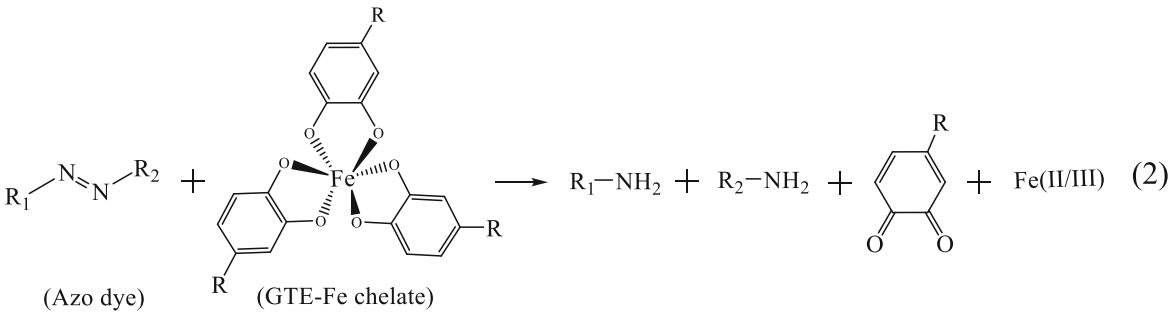

Discussion

In this study, efficient decolorization of azo dyes via in situ generation of GTE-Fe chelate was reported for the first time. More than 90% azo dye decolorization efficiency could be achieved under the anaerobic condition. Compared with other decolorization technology, in situ generation of GTE-Fe chelate for azo dye decolorization is competitive and promising due to its advantages of low cost, ease in operation and scale-up, and high efficiency. Various biological processes are generally employed to treat a mass of dyeing wastewaters (Hadibarata et al. 2012; Pan et al. 2014; Santal et al. 2011). However, these bioprocesses normally require longer HRT (hydraulic retention time), as well as extra energy-intensive aeration and provision of nutrients, to achieve designed decolorization efficiency (Fu and Viraraghavan 2001; Khan et al. 2013). In addition, biosorption occurred during these biological processes could negatively affect the decolorization efficiency due to the biotoxicity of azo dye molecules to living microorganism cells (Oztürk and Abdullah 2006). By contrast, in situ generation of GTE-Fe chelate for azo dye decolorization is suitable for treating a wide range of azo dye concentrations. To enhance the biodecolorization efficiency, various active functional enzymes including laccase, manganese peroxidase, and lignin peroxidase from microorganisms were utilized as biodecolorants (Alam et al. 2009; Cheng et al. 2007; GS et al. 2002). However, the enzyme activity could be inhibited by the metal (e.g., Fe) ions in the dyeing wastewaters (Murugesan et al. 2009). On the contrary, during GTE-Fe chelate decolorization process, some metal ions, such as

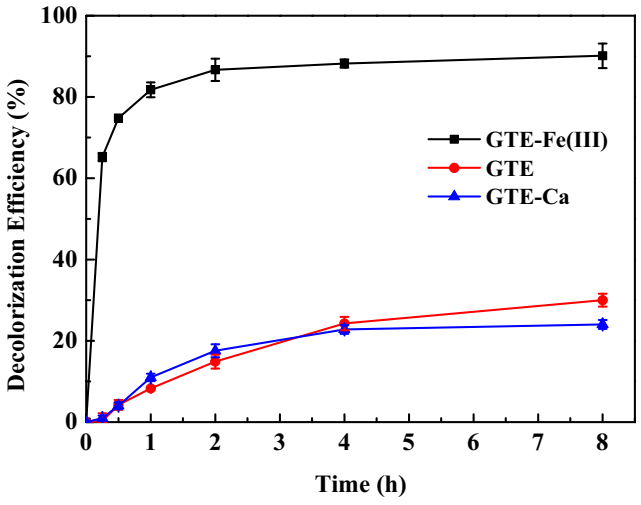

Fig. 8 Bridging effects of metal cations on AO7 decolorization. The concentrations of AO7, calcium ions, Fe(III) ions, and green tea extract (GTE) in the experiment are 50 mg/L, 357 mg-Ca/L, 500 mg-Fe/L, and 6.67 g-GT/L, respectively

iron and copper ions, in the dyeing wastewaters could form organometal chelates and enhance the decolorization performance. As for abiotic decolorization processes, in situ-generated GTE-Fe chelate have higher decolorization efficiency and rate than other reductive decolorants (e.g., zero valent iron particles) (Khan et al. 2017). One possible reason is the well dispersion of the in situ-generated GTE-Fe chelate and thus accelerates the reaction between azo dyes and reducing equivalents. Additionally, reductive activities of the zero valent iron particles will be compromised by generation and deposition of iron oxyhydroxides, e.g., Fe_3O_4, $Fe(OH)_3$, and Fe_2O_3, on the particle surface (Khan et al. 2017). Moreover, compared with oxidative decolorization processes using strong oxidants (e.g., ozone, chlorine, and H_2O_2), the azo dye decolorization by in situ-generated GTE-Fe chelate is more economic and suitable for practical application in the treatment of dyeing wastewaters (Elmorsi et al. 2010; Mijin et al. 2012; Sharma et al. 2013).

Polyphenols as biodegradable natural polymers in GTE are well known for their antioxidant activities, and their reducing ability has been widely reported. For instance, GTE was applied to synthesize iron-based nanoparticles (Akhavan et al. 2012; Chrysochoou et al. 2012; Klimczak et al. 2007; Lu and Foo 2001; Markova et al. 2014; Weng et al. 2013). Nonetheless, controversial conclusions on the iron redox status (Fe^{2+} vs. Fe^0) were proposed, due to the high reactivity of GTE-reduced irons to oxygen during the test of iron redox status (Hoag et al. 2009; Markova et al. 2014; Wang et al. 2015). It is well known that polyphenol compounds are effective metal chelators (Andjelković et al. 2006; Hider et al. 2001). Fe(III)-polyphenol chelate was found to be more stable than Fe(II) (Perron and Brumaghim 2009). In this study, the efficient azo dye decolorization via GTE-Fe chelate was shown to be due to the enhancement of deprotonation of hydroxyl groups of polyphenols in GTE by ferric ions. The deprotonated polyphenols further attack the azo bonds to achieve decolorization of azo dyes. Meanwhile, a certain amount of ferric ions can be reduced to ferrous ions by polyphenols which can also participate in the decolorization of azo dye. This is confirmed by the results of XPS analysis (Fig. 5) and the decolorization of azo dye in the presence of ferrous ions (Fig. 2). Moreover, as shown in Fig. 2, the decolorization efficiency of GTE-Fe(II) was much higher than Fe(II), the reason for that should be because the binding of polyphenol ligands to ferric ions lowers the reduction potential of iron and enhances the rate of ferric ions oxidation (Hajji et al. 2006). After the reductive cleavage of azo bonds, polyphenols in GTE-Fe chelate will exist as benzoquinone-like forms, which will probably be separated from GTE-Fe chelate without coordinate bonds with iron ions (Akhavan et al. 2012). Therefore, influence of oxidation products of GTE-Fe chelate in subsequent decolorization would be negligible. Based on the decolorization mechanism of GTE-Fe chelate, the reducing capability of polyphenols in GTE is critical. Compared with fermented black tea and Oolong tea, green tea might be better for in situ generation of GTE-Fe chelate for azo dye decolorization, due to the higher constitution of reducing equivalents reserved in green tea (Graham 1992). Nonetheless, whether the fresh tea leaf could be utilized as an alternative to GTE to further improve the azo dye decolorization process still warrants future studies.

Conclusions

An easy and efficient method for azo dye decolorization was developed in this study. The in situ-generated GTE-Fe(III) chelate could decolorize > 80% of two typical azo dyes (AO7 and AB1) in the first 30 min under anaerobic conditions. During the decolorization, the hydroxyl groups in green tea polyphenols (main components of GTE) are ready to be deprotonated and act as nucleophiles, which further attack azo bonds. The presence of iron ions could promote the deprotonation of hydroxyl groups, resulting in the enhancement of azo dye decolorization.

Acknowledgements This study was supported by the Guangzhou Science and Technology Program general project (201804010141).

References

Aboulhassan MA, Souabi S, Yaacoubi A, Baudu M (2006) Improvement of paint effluents coagulation using natural and synthetic coagulant aids. J Hazard Mater 138:40–45

Akhavan O, Kalaee M, Alavi ZS, Ghiasi SMA, Esfandiar A (2012) Increasing the antioxidant activity of green tea polyphenols in the presence of iron for the reduction of graphene oxide. Carbon 50: 3015–3025

Alam MZ, Mansor MF, Jalal KC (2009) Optimization of decolorization of methylene blue by lignin peroxidase enzyme produced from sewage sludge with Phanerocheate chrysosporium. J Hazard Mater 162: 708–715

Amjad Ali K, Qayyum H (2007) Potential of plant polyphenol oxidases in the decolorization and removal of textile and non-textile dyes. J Environ Sci 19:396–402

Andjelković M, Van Camp J, De Meulenaer B, Depaemelaere G, Socaciu C, Verloo M, Verhe R (2006) Iron-chelation properties of phenolic acids bearing catechol and galloyl groups. Food Chem 98:23–31

Barreto-Rodrigues M, Silveira J, Zazo JA, Rodriguez JJ (2016) Synthesis, characterization and application of nanoscale zero-valent iron in the degradation of the azo dye Disperse Red 1. J. Environ. Chem Eng 5:628–634

Barth G, Linder R, Bryson C (1988) Advances in charge neutralization for XPS measurements of nonconducting materials. Surf Interface Anal 11:307–311

Beamson G, Briggs D (1992) High resolution XPS of organic polymers. Wiley

Biesinger MC, Payne BP, Grosvenor AP, Lau LW, Gerson AR, Smart RSC (2011) Resolving surface chemical states in XPS analysis of first row transition metals, oxides and hydroxides: Cr, Mn, Fe, Co and Ni. Appl Surf Sci 257:2717–2730

Blomquist J, Helgeson U, Moberg LC, Folkesson B, Larsson R (1983) ESCA and Mössbauer spectra of some iron (III) betadiketonates and tetraphenylporphyrin iron (III) chloride. Inorg Chim Acta 69:17–23

Cheng X, Jia R, Li P, Tu S, Zhu Q, Tang W, Li X (2007) Purification of a new manganese peroxidase of the white-rot fungus Schizophyllum sp. F17, and decolorization of azo dyes by the enzyme. Enzyme Microb Tech 41:258–264

Chrysochoou M, Johnston CP, Dahal G (2012) A comparative evaluation of hexavalent chromium treatment in contaminated soil by calcium polysulfide and green-tea nanoscale zero-valent iron. J Hazard Mater 201–202:33–42

Cui M-H, Cui D, Gao L, Wang A-J, Cheng H-Y (2016a) Azo dye decolorization in an up-flow bioelectrochemical reactor with domestic wastewater as a cost-effective yet highly efficient electron donor source. Water Res 105:520–526

Cui MH, Cui D, Hyung-Sool L, Liang B, Wang AJ, Cheng HY (2016b) Effect of electrode position on azo dye removal in an up-flow hybrid anaerobic digestion reactor with built-in bioelectrochemical system. Sci Rep 6:25223

Elmorsi TM, Riyad YM, Mohamed ZH, Hm AEB (2010) Decolorization of Mordant red 73 azo dye in water using H2O2/UV and photo-Fenton treatment. J Hazard Mater 174:352–358

Fang Z, Song HL, Cang N, Li XN (2013) Performance of microbial fuel cell coupled constructed wetland system for decolorization of azo dye and bioelectricity generation. Bioresour Technol 144:165–171

Fu Y, Viraraghavan T (2001) Fungal decolorization of dye wastewaters: a review. Bioresour Technol 79:251–262

Graham HN (1992) Green tea composition, consumption, and polyphenol chemistry. Prev Med 21:334–350

Grinberg LN, Newmark H, Kitrossky N, Rahamim E, Chevion M, Rachmilewitz EA (1997) Protective effects of tea polyphenols against oxidative damage to red blood cells. Biochem Pharmacol 54:973–978

GS N JG, GM G RZ, J R WS (2002) Decolorization of textile dyes by laccases from a newly isolated strain of Trametes modesta. Water Res 36:1449–1456

Hadibarata T, Yusoff ARM, Kristanti RA (2012) Decolorization and metabolism of anthraquionone-type dye by laccase of white-rot fungi Polyporus sp. S133. Water Air Soil Poll 223:933–941

Hajji HE, Nkhili E, Tomao V, Dangles O (2006) Interactions of quercetin with iron and copper ions: complexation and autoxidation. Free Radic Res 40:303–320

Hider RC, Liu ZD, Khodr HH (2001) Metal chelation of polyphenols, Methods Enzymol Elsevier, pp. 190–203

Hoag GE, Collins JB, Holcomb JL, Hoag JR, Nadagouda MN, Varma RS (2009) Degradation of bromothymol blue by 'greener' nano-scale zero-valent iron synthesized using tea polyphenols. J Mater Chem 19:8671–8677

Huang L, Weng X, Chen Z, Megharaj M, Naidu R (2014) Green synthesis of iron nanoparticles by various tea extracts: comparative study of the reactivity. Spectrochim Acta A 130:295–301

Imran M, Arshad M, Negm F, Khalid A, Shaharoona B, Hussain S, Mahmood Nadeem S, Crowley DE (2016) Yeast extract promotes decolorization of azo dyes by stimulating azoreductase activity in Shewanella sp. strain IFN4. Ecotox Environ Safe 124:42–49

Khan R, Bhawana P, Fulekar MH (2013) Microbial decolorization and degradation of synthetic dyes: a review. Rev Environ Sci Bio 12:75–97

Khan A, Prabhu SM, Park J, Lee W, Chon C-M, Ahn JS, Lee G (2017) Azo dye decolorization by ZVI under circum-neutral pH conditions and the characterization of ZVI corrosion products. J Ind Eng Chem 47:86–93

Klimczak I, Malecka M, Szlachta M, Gliszczynskaswiglo A (2007) Effect of storage on the content of polyphenols, vitamin C and the antioxidant activity of orange juices. J Food Compos Anal 20:313–322

Lee YH, Pavlostathis SG (2004) Decolorization and toxicity of reactive anthraquinone textile dyes under methanogenic conditions. Water Res 38:1838–1852

Li HX, Xu B, Tang L, Zhang JH, Mao ZG (2015) Reductive decolorization of indigo carmine dye with Bacillus sp. MZS10. Int Biodeter Biodegr 103:30–37

Lu Y, Foo LY (2001) Antioxidant activities of polyphenols from sage (Salvia officinalis). Food Chem 75:197–202

Markova Z, Novak P, Kaslik J, Plachtova P, Brazdova M, Jancula D, Siskova KM, Machala L, Marsalek B, Zboril R (2014) Iron(II,III)–polyphenol complex nanoparticles derived from green tea with remarkable ecotoxicological impact. ACS Sustain Chem Eng 2:1674–1680

Melidou M, Riganakos K, Galaris D (2005) Protection against nuclear DNA damage offered by flavonoids in cells exposed to hydrogen peroxide: the role of iron chelation. Free Radical Bio Med 39:1591–1600

Mijin DŽ, Ivić MLA, Onjia AE, Grgur BN (2012) Decolorization of textile dye CI Basic Yellow 28 with electrochemically generated active chlorine. Chem Eng J 204–206:151–157

Moulton MC, Braydich-Stolle LK, Nadagouda MN, Kunzelman S, Hussain SM, Varma RS (2010) Synthesis, characterization and biocompatibility of "green" synthesized silver nanoparticles using tea polyphenols. Nano 2:763–770

Murugesan K, Kim Y-M, Jeon J-R, Chang Y-S (2009) Effect of metal ions on reactive dye decolorization by laccase from Ganoderma lucidum. J Hazard Mater 168:523–529

Nanjo F, Goto K, Seto R, Suzuki M, Sakai M, Hara Y (1996) Scavenging effects of tea catechins and their derivatives on 1,1-diphenyl-2-picrylhydrazyl radical. Free Radical Bio. Med. 21:895–902

Nune S, Chanda N, Shukla R, Katti K, Kulkarni R, Thilakavathy S, Mekapothula S, Kannan R (2009) Green nanotechnology from tea: phytochemicals in tea as building blocks for production of biocompatible gold nanoparticles. J Mater Chem 19:2912–2920

Oztürk A, Abdullah MI (2006) Toxicological effect of indole and its azo dye derivatives on some microorganisms under aerobic conditions. Sci Total Environ 358:137–142

Pagga U, Brown D (1986) The degradation of dyestuffs: part II behaviour of dyestuffs in aerobic biodegradation tests. Chemosphere 15:479–491

Pan K, Zhao N, Yin Q, Zhang T, Xu X, Fang W, Hong Y, Fang Z, Xiao Y (2014) Induction of a laccase Lcc9 from Coprinopsis cinerea by fungal coculture and its application on indigo dye decolorization. Bioresour Technol 162:45–52

Perron NR, Brumaghim JL (2009) A review of the antioxidant mechanisms of polyphenol compounds related to iron binding. Cell Biochem Biophys 53:75–100

Rathod J, Dhebar S, Archana G (2017) Efficient approach to enhance whole cell azo dye decolorization by heterologous overexpression of Enterococcus sp. L2 azoreductase (azoA) and Mycobacterium vaccae formate dehydrogenase (fdh) in different bacterial systems. Int Biodeter Biodegr. Int. Biodeter. Biodegr 124:91–100

Rawat D, Mishra V, Sharma RS (2016) Detoxification of azo dyes in the context of environmental processes. Chemosphere 155:591–605

Salah N, Miller NJ, Paganga G, Tijburg L, Bolwell GP, Rice-Evans C (1995) Polyphenolic flavanols as scavengers of aqueous phase radicals and as chain-breaking antioxidants. Arch Biochem Biophys 322:339–346

Santal AR, Singh NP, Saharan BS (2011) Biodegradation and detoxification of melanoidin from distillery effluent using an aerobic bacterial strain SAG 5 of Alcaligenes faecalis. J Hazard Mater 193:319–324

Serafini M, Ghiselli A, Ferroluzzi A (1996) In vivo antioxidant effect of green and black tea in man. Eur J Clin Nutr 50:28

Sharma S, Buddhdev J, Patel M, Ruparelia JP (2013) Studies on degradation of reactive red 135 dye in wastewater using ozone. Procedia Eng 51:451–455

Srivastava S, Badrinarayanan S, Mukhedkar A (1985) X-ray photoelectron spectra of metal complexes of substituted 2, 4-pentanediones. Polyhedron 4:409–414

Stolz A (2001) Basic and applied aspects in the microbial degradation of azo dyes. Appl Microbiol Biot 56:69–80

Tan BJ, Klabunde KJ, Sherwood PM (1990) X-ray photoelectron spectroscopy studies of solvated metal atom dispersed catalysts. Monometallic iron and bimetallic iron-cobalt particles on alumina. Chem Mater 2:186–191

Vinodgopal K, Wynkoop DE, Kamat PV (1996) Environmental photochemistry on semiconductor surfaces: photosensitized degradation of a textile azo dye, Acid Orange 7, on TiO2 particles using visible light. Environ Sci Technol 30:1660–1666

Wang Z, Fang C, Mallavarapu M (2015) Characterization of iron–polyphenol complex nanoparticles synthesized by Sage (Salvia officinalis) leaves. Environ Technol Innov 4:92–97

Weng X, Huang L, Chen Z, Megharaj M, Naidu R (2013) Synthesis of iron-based nanoparticles by green tea extract and their degradation of malachite. Ind Crop Prod 51:342–347

Wilson D, Langell MA (2014) XPS analysis of oleylamine/oleic acid capped Fe3O4 nanoparticles as a function of temperature. Appl Surf Sci 303:6–13

Zaveri NT (2006) Green tea and its polyphenolic catechins: medicinal uses in cancer and noncancer applications. Life Sci 78:2073–2080

Zhang S-J, Yu H-Q, Li Q-R (2005) Radiolytic degradation of Acid Orange 7: a mechanistic study. Chemosphere 61:1003–1011